Microwave spectroscopy of S, P, and D states of sodium Rydberg atoms

S. Dyubko, M. Efimenko, V. Efremov, and S. Podnos
Laboratory of Molecular Spectroscopy, Department of Radiophysics, Kharkov State University, Svobody sq., 4, Kharkov, Ukraine, 310077
(Received 5 January 1995)

The transition frequencies of the $nS \rightarrow nP$ and $nD \rightarrow (n+1)P$ sodium atom series were measured within the 53–350-GHz range for the main quantum number $n=22$–32. More precise values of *ls* splitting and quantum defects for $P_{1/2,3/2}$ and $D_{3/2,5/2}$ terms were determined. The frequencies were measured with an accuracy of better than 50 kHz. The results were treated using the Rydberg formula $E(n,l,j)=-R_{\mathrm{Na}}/(n-\delta_{nlj})^2$. The quantum defect was calculated by using the expression $\delta_{nj}=\varepsilon_{lj}+\alpha_{lj}/n^{*2}$. The constants ε_{lj} and α_{lj} that result from this work are $\varepsilon_{1/2}=0.855\,444\,58(14)$, $\alpha_{1/2}=0.112\,668\,(90)$, $\varepsilon_{3/2}=0.854\,625\,83(12)$, and $a_{3/2}=0.112\,878(81)$ for the P term and $\varepsilon_{3/2}=0.014\,909\,19(38)$, $a_{3/2}=-0.042\,19(25)$, $\varepsilon_{5/2}=0.014\,925\,82(55)$, and $a_{5/2}=-0.043\,33(35)$ for the D term. The *ls*-splitting constants determined from the expression $\Delta\nu_l=A_l/n^{*3}$ are $A_p=5\,384\,790(420)$ MHz for the P term and $A_d=97\,340(680)$ MHz for the D term.

PACS number(s): 32.80.Rm, 33.80.Rv

INTRODUCTION

There have been some reports [1–6] on the spectroscopy of Na I Rydberg states, on the development of spectroscopic techniques in this field, and on the investigation of both *ls* splitting and the quantum-defect variation for terms with low l. The most striking of them is the paper [5] that contains information on precise investigation of the S term by the method of two-photon spectroscopy.

We have created an atom-beam radiospectrometer and measured the transition frequencies of the S, P, and D states of a highly excited sodium atom. Our results completely confirm the known frequency values of two-photon transitions of the $nS_{1/2} \rightarrow (n+1)S_{1/2}$ type [5] and are in good agreement with the energy levels of the S states obtained from the quantum-defect values determined in [5]. However, the measurements of $nS \rightarrow nP$ and especially $nD \rightarrow (n+1)P$ transition frequencies revealed an essential discrepancy between both frequencies observed in [3,5] and the ones calculated by quantum-defect constants reported in [5].

We have diminished considerably the width of the observed resonances of $nS \rightarrow nP$ type and especially of $nD \rightarrow (n+1)P$ type by means of the removal of residual fields in the region of the Rydberg-atom–microwave interaction. We obtained more precise values of the quantum defect for P and D terms, and measured the fine-structure splitting of these terms.

EXPERIMENTAL DETAILS

We populated the Na atom Rydberg states by the known two-step excitation methods

$$3S_{1/2} \rightarrow 3P_{1/2,3/2} \rightarrow nS_{1/2}$$

or

$$3S_{1/2} \rightarrow 3P_{1/2,3/2} \rightarrow nD_{5/2,3/2} \ .$$

Tunable dye lasers were used as sources of excitation. The dye lasers are pumped by a N_2 laser with a pulse repetition rate of 25 Hz and pulse duration of 5 ns.

The atom beam is formed by a 5×0.3 mm^2 rectangular slit cut out in a cell that contains a drop of Na heated up to 180 °C. A pressure of residual gases of 5×10^{-7} Torr is provided by an oil-diffusion pump with a nitrogen-cooled trap. The atom beam is excited inside an ionization capacitor. The distance between the beam source and the point of excitation is 15 cm. The dimensions of the capacitor plates are 40×40 mm^2 and their clearance is 6.5 mm. Free electrons are detected by a channel electron multiplier spaced on the back side of one of the capacitor plates. This plate has a number of channels with a diameter of 0.4 mm and a length of 4 mm through which the electrons enter into the multiplier input. Such a construction provides reliable shielding of the Rydberg atoms against the multiplier electrostatic field but weakens the effective signal essentially.

We used lasers with a narrow width of output radiation and with a high power stability to improve the signal-to-noise relation. Also, we carefully tuned the time intervals for the excitation process and chose the optimal regime of the electron multiplier. However, the most effective way to increase the signal-to-noise relation was to accumulate and average by computer the results of the measurements.

We have minimized the external electromagnetic interferences inside the ionization capacitor space by using a special construction of dc rf connectors, then carefully shielding the conductors inside the cell, and finally by using low-resistance shunting of the ionization capacitor plates. However, in spite of that we have found the existence of a stray electrostatic field in the interaction region for some experimental conditions. The presence of this stray field was revealed as a disturbance of the resonance form and as a frequency shift of the top of the resonance. We have found a correlation between the presence of the stray field and the location of the Na film that

was deposited on the ionization capacitor surfaces. This leads to the appearance of a weak inhomogeneous electrostatic field inaccessible for direct measurement. The stray electrostatic field occurred 20–60 min after the start of the heating of the atom-beam source. For this reason, reliable measurements were possible either in the short time after the start of the experiment, or after the intentional deposition of a homogeneous film of Na atoms on the ionization capacitor plates. In both cases, the disturbance of the resonance form and frequency shift was minimal.

The level of stray and residual fields was always checked before the transition-frequency measurement. In order to check the residual-field level, we supplied the dc potential $\delta U = 20-100$ mV to the capacitor plates and then recorded the resonance for the opposite polarity of applied potential. The values of the frequency shifts are the same and independent of applied-potential polarity in the case when parasitic and residual fields are absent or when their values are negligible. Such behavior of the transition-frequency shift is stipulated by the quadratic Stark effect in weak electrostatic fields.

The Rydberg-state microwave transitions are induced by radiation of a microwave-frequency synthesizer (53–80 GHz) or its harmonics up to the sixth. The spectrum width of the synthesizer radiation does not exceed $n \times 7.5$ kHz, where n is the number of the harmonic of the output radiation. The synthesizer is controlled by the computer.

Spectra are recorded in the following way. A N_2 laser starts up the rhodamine-6*G* and violet range dye lasers. The delay between radiation pulses of the dye lasers is 3

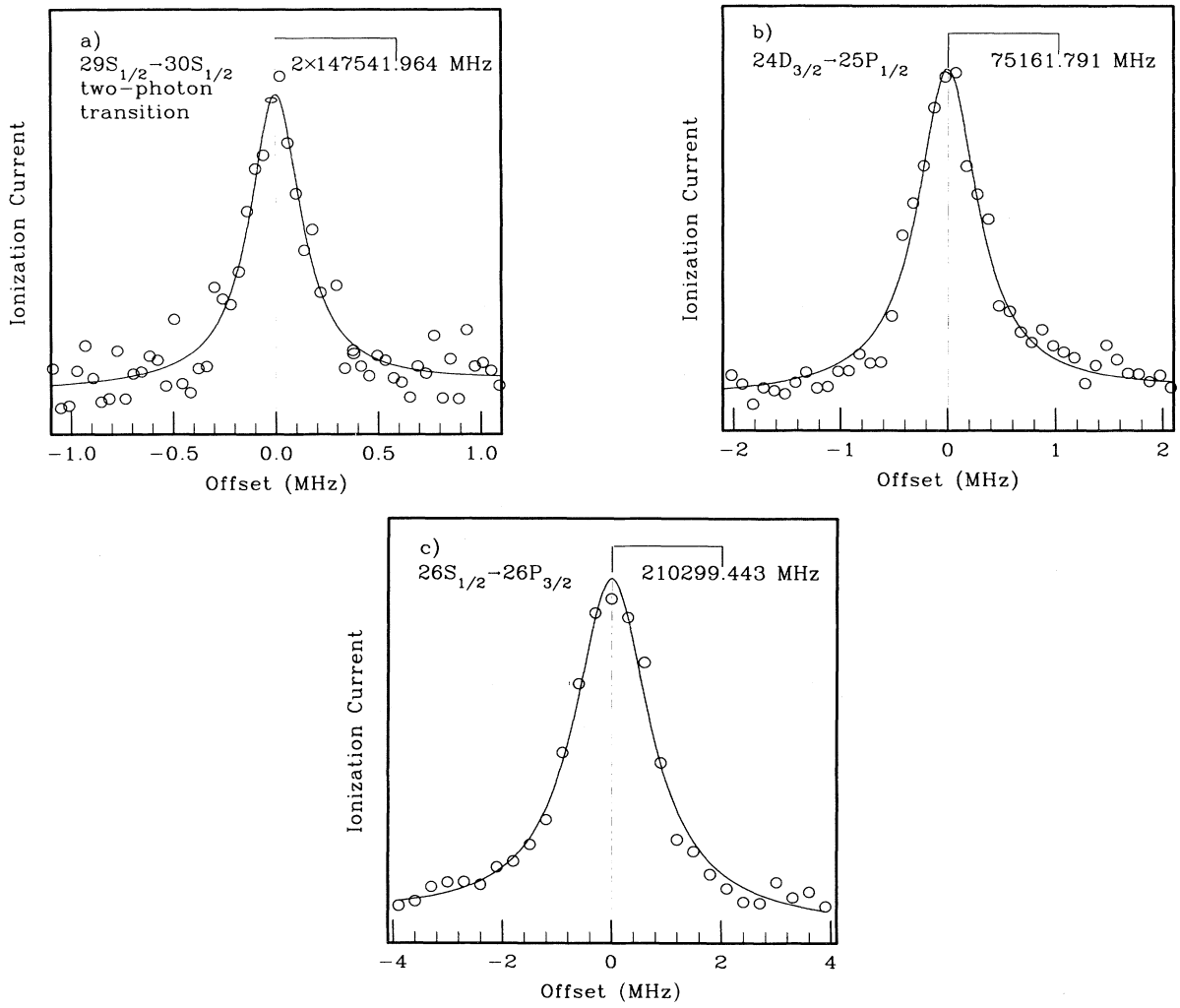

FIG. 1. Examples of the observed microwave resonances for NaI in the Rydberg states: (a) two-photon resonance of $29S_{1/2} \rightarrow 30S_{1/2}$ type; (b) single-photon resonance of $24D_{3/2} \rightarrow 25P_{1/2}$ type; (c) single-photon resonance of $26_{1/2} \rightarrow 26P_{3/2}$ type. The unfilled points are ensemble-averaged (over 400 measurements per point) results at fixed frequencies varied with the step of 100 kHz. The solid curve is the optimum approximation of the resonance by a Lorentz contour. The transition frequency was determined as the contour top. The ordinate corresponds to the transition intensity in arbitrary units of the linear scale.

ns. The laser beams were carefully merged into one and were focused into the atom-beam region between the ionization capacitor plates. The excited Na atoms are ionized just at the moment when they are passing the electron multiplier inlets. The interaction between the considerably weakened microwave radiation and Rydberg atoms occurs in the time period between the creation of Rydberg atoms and their ionization. The ionization of Rydberg atoms is induced by the voltage pulse supplied to the ionization capacitor plates. The amplitude of this pulse is rigorously determined for a given Rydberg state. The delay of the ionization pulse with respect to the creation of Rydberg atoms is 1.5–3 μs. So the resonance width in our case is determined generally by the time of interaction between the Rydberg atoms and the microwave field and does not exceed 1 MHz.

Selected spectrum lines of the Na atom Rydberg states are shown in Fig. 1.

TABLE I. Experimental values (in MHz) for the transition frequencies $|nlj\rangle \rightarrow |n'l'j'\rangle$ observed for NaI. The discrepancies between the experimental and calculated values of transition frequencies are shown as δF.

n	Transition type	Frequency (MHz)	δF (MHz)
1	$22S_{1/2} \rightarrow 22P_{3/2}$	355 650.72	0.03
2	$22S_{1/2} \rightarrow 22P_{1/2}$	355 081.20	0.03
3	$23S_{1/2} \rightarrow 23P_{3/2}$	309 116.83	−0.23
4	$23S_{1/2} \rightarrow 23P_{1/2}$	308 621.29	−0.50
5	$24S_{1/2} \rightarrow 24P_{3/2}$	270 359.26	0.02
6	$24S_{1/2} \rightarrow 24P_{1/2}$	269 925.03	−0.05
7	$25S_{1/2} \rightarrow 25P_{3/2}$	237 819.13	0.61
8	$25S_{1/2} \rightarrow 25P_{1/2}$	237 437.20	−0.02
9	$26S_{1/2} \rightarrow 26P_{3/2}$	210 299.44	−0.02
10	$26S_{1/2} \rightarrow 26P_{1/2}$	209 960.69	0.02
11	$27S_{1/2} \rightarrow 27P_{3/2}$	186 866.71	0.00
12	$27S_{1/2} \rightarrow 27P_{1/2}$	186 565.42	−0.03
13	$28S_{1/2} \rightarrow 28P_{3/2}$	166 790.05	−0.06
14	$28S_{1/2} \rightarrow 28P_{1/2}$	166 520.74	0.01
15	$29S_{1/2} \rightarrow 29P_{3/2}$	149 489.37	−0.02
16	$29S_{1/2} \rightarrow 29P_{1/2}$	149 247.75	0.04
17	$30S_{1/2} \rightarrow 30P_{3/2}$	134 501.02	0.04
18	$30S_{1/2} \rightarrow 30P_{1/2}$	134 283.49	0.03
19	$31S_{1/2} \rightarrow 31P_{3/2}$	121 451.35	0.00
20	$31S_{1/2} \rightarrow 31P_{1/2}$	121 254.75	0.01
21	$32S_{1/2} \rightarrow 32P_{3/2}$	110 036.67	0.01
22	$32S_{1/2} \rightarrow 32P_{1/2}$	109 858.45	−0.04
23	$29S_{1/2} \rightarrow 30S_{1/2}$	2×147 541.96	−0.02
24	$24D_{5/2} \rightarrow 25P_{3/2}$	75 551.33	−0.02
25	$24D_{3/2} \rightarrow 25P_{3/2}$	75 544.35	−0.03
26	$24D_{3/2} \rightarrow 25P_{1/2}$	75 161.79	−0.02
27	$25D_{5/2} \rightarrow 26P_{3/2}$	66 873.30	0.01
28	$25D_{3/2} \rightarrow 26P_{3/2}$	66 867.01	0.05
29	$25D_{3/2} \rightarrow 26P_{1/2}$	66 528.35	0.00
30	$26D_{5/2} \rightarrow 27P_{3/2}$	59 474.72	0.05
31	$26D_{3/2} \rightarrow 27P_{3/2}$	59 469.22	−0.05
32	$26D_{3/2} \rightarrow 27P_{1/2}$	59 167.79	0.06
33	$27D_{5/2} \rightarrow 28P_{3/2}$	53 128.40	−0.03
34	$27D_{3/2} \rightarrow 28P_{3/2}$	53 123.34	−0.01
35	$27D_{3/2} \rightarrow 28P_{1/2}$	52 854.10	−0.01

TABLE II. Quantum-defect coefficients obtained from our high-resolution spectroscopy results.

Type of term	ε_{lj}	a_{lj}
$nS_{1/2}$	1.347 969 2(4)[a]	0.061 37(10)[a]
$nP_{1/2}$	0.855 444 58(14)	0.112 668(90)
$nP_{3/2}$	0.854 625 83(12)	0.112 878(81)
$nD_{3/2}$	0.014 909 19(38)	−0.042 19(25)
$nD_{5/2}$	0.014 925 82(55)	−0.043 33(35)

[a]Values calculated by [5].

RESULTS AND DISCUSSION

The results of the measurements are listed in Table I. 22 frequencies of the single-photon transitions of $nS \rightarrow nP$ type and 12 of the transitions of $nD \rightarrow nP$ type were measured. Also, we measured the frequency value of a two-photon transition $29S \rightarrow 30S$.

The energy levels of a Na atom for various quantum-number values n, l, and j were calculated using the Rydberg formula

$$E(n,l,j) = -R_{\mathrm{Na}}/n^{*2} = -R_{\mathrm{Na}}/(n-\delta_{nlj})^2 , \qquad (1)$$

where $R_{\mathrm{Na}} = 3\,289\,763\,408(20)$ MHz. The first two terms of the iteration formula

$$\delta_{nlj} = \varepsilon_{lj} + a_{lj}/n^{*2} + \cdots \qquad (2)$$

were used for quantum-defect determination. The coefficients ε_{lj} and a_{lj} corresponding to P and D terms

TABLE III. Fine splitting (in MHz) of NaI levels observed in our experiment. The values of fine splitting were calculated by using the formulas (1) and (3). δf_1 and δf_2 are the discrepancies between the observed and calculated values of the fine splitting, respectively.

n	The type of splitting level	f_{obs} (MHz)	δf_1 (MHz)	δf_2 (MHz)
1	$22P_{1/2} \leftrightarrow 22P_{3/2}$	569.52	0.01	−0.08
2	$23P_{1/2} \leftrightarrow 23P_{3/2}$	495.54	−0.27	−0.32
3	$24P_{1/2} \leftrightarrow 24P_{3/2}$	434.23	−0.07	−0.09
4	$25P_{1/2} \leftrightarrow 25P_{3/2}$	381.93	−0.63	−0.64
5	$25P_{1/2} \leftrightarrow 25P_{3/2}$	382.56[a]	0.01	0.00
6	$26P_{1/2} \leftrightarrow 26P_{3/2}$	338.76	0.04	0.05
7	$26P_{1/2} \leftrightarrow 26P_{3/2}$	338.66[a]	−0.04	−0.04
8	$27P_{1/2} \leftrightarrow 27P_{3/2}$	301.29	−0.03	−0.02
9	$27P_{1/2} \leftrightarrow 27P_{3/2}$	301.43[a]	0.11	0.12
10	$28P_{1/2} \leftrightarrow 28P_{3/2}$	269.31	0.07	0.09
11	$28P_{1/2} \leftrightarrow 28P_{3/2}$	269.24[a]	0.00	0.02
12	$29P_{1/2} \leftrightarrow 29P_{3/2}$	241.72	0.16	0.19
13	$30P_{1/2} \leftrightarrow 30P_{3/2}$	217.53	−0.01	0.01
14	$31P_{1/2} \leftrightarrow 31P_{3/2}$	196.61	0.01	0.03
15	$32P_{1/2} \leftrightarrow 32P_{3/2}$	178.22	−0.05	−0.03
16	$24D_{5/2} \leftrightarrow 24D_{3/2}$	6.98	0.00	−0.08
17	$25D_{5/2} \leftrightarrow 25D_{3/2}$	6.29	0.05	0.05
18	$26D_{5/2} \leftrightarrow 26D_{3/2}$	5.51	−0.09	−0.04
19	$27D_{5/2} \leftrightarrow 27D_{3/2}$	5.06	0.02	0.11

[a]Obtained from $nD \rightarrow (n+1)P$ transitions.

were calculated from our experimental results using the quantum-defect value for the S term obtained in [5]. Calculations were carried out by the least-squares fitting method. The corresponding values of coefficients ε_{lj} and a_{lj} are listed in Table II.

The comparison of the calculated transition frequencies with the observed ones shows good agreement with the exception of three transitions. They are $23S_{1/2} \rightarrow 23P_{1/2,3/2}$ and $25S_{1/2} \rightarrow 25P_{1/2}$ transitions. In this case, as one can see from Table I, the agreement is an order of magnitude worse. The reasons for the given discrepancy have not been determined yet.

The transition frequencies obtained in [5] are shifted with respect to ours by 1 MHz at least for $nS \rightarrow nP$-type transitions and up to tens of MHz for $nD \rightarrow (n+1)P$-type transitions. In our opinion, residual electric fields occurred in the experimental setup [5]. This leads to the Stark shift of the transition frequency to the high-frequency region. The higher accuracy of our frequency measurements of $nS \rightarrow nP$ and $nD \rightarrow (n+1)P$ transition types was achieved due to the significant decrease of residual fields inside the interaction region, the application of the microwave synthesizer with a narrow width of output radiation, and the increased signal-to-noise relation.

The values of fine splitting of the P and D terms are shown in Table III. The frequency values corresponding to the fine splitting can be represented as a series

$$\Delta\nu_l = A_l/n^{*3} + B_l/n^{*5} + \ldots , \tag{3}$$

where A and B are constants. Since the principal quantum number n in our experiments was greater than 20, only the first term can remain in this series. In this case, the values of the constants are $A_p = 5\,384\,790(420)$ MHz for the P term and $A_d = 97\,340(680)$ MHz for the D term. Also, the residuals δf_1 and δf_2 between the measured values of fine splitting and those obtained by formula (1) and formula (3), respectively, are shown in Table III.

Unfortunately, we could not decrease the residual fields in the interaction region to such an extent that it would be possible to observe the transitions between the levels with quantum numbers $l > 2$ without frequency shift and broadening. We hope to decrease the residual fields in the future with a new spectrometer cell in which the precipitation of the Na film will be prevented. Another factor restricting the frequency resolution and accuracy of the measurements is the short interaction time between the atoms and the microwave field. It is assumed that the Ramsay method and deep cooling of the camera walls will be used in order to increase the interaction time in a new construction of the spectrometer and we hope to achieve much higher resolution in the investigation of the spectrum of Rydberg atoms with $l > 2$.

ACKNOWLEDGMENTS

The authors are deeply obliged to V. Gerasimov for many helpful discussions. This work was supported, in part, by a Soros Foundation Grant awarded by the American Physical Society APS137.

[1] W. E. Cooke, T. F. Gallagher, R. M. Hill, and S. A. Edelstein, Phys. Rev. A **16**, 2473 (1977).

[2] T. F. Gallagher, L. M. Humphrey, R. M. Hill, W. E. Cooke, and S. A. Edelstein, Phys. Rev. A **15**, 1937 (1977).

[3] C. Fabre, S. Haroche, and P. Goy, Phys. Rev. A **18**, 229 (1978).

[4] C. Fabre, S. Haroche, and P. Goy, Phys. Rev. A **22**, 778 (1980).

[5] C. Fabre, Ann. Phys. (Paris) **4**, 247 (1982).

[6] I. M. Beterov, A. O. Vyrodov, I. I. Ryabtsev, and N. V. Fateev, Zh. Eksp. Teor. Fiz. **101**, 1154 (1992).